

# TCP traffic is multifractal: a numerical study.

**Rudolf H. Riedi**

Rice University, Dept. ECE, MS 366  
6100 Main Street, Houston TX 77005 - 1892  
email: riedi@rice.edu

and

**Jacques Lévy Véhel**

Projet Fractales, INRIA Rocquencourt,  
B.P. 105, 78153 Le Chesnay Cedex, France  
email: jlv@bora.inria.fr

Revised and condensed version of INRIA Research Report 3129

Rice University, October 1997

## Abstract

The apparent ‘fractal’ properties of TCP data traffic have recently attracted considerable interest. Most prominently, fractional Brownian motion (FBM) has been used to model the long range dependence of traffic traces through *self-similarity*. Traffic being by nature a process of positive increments, though, a *multifractal* approach appears more natural. In this study, various traces of TCP traffic have been analyzed from both points of view. Though evidence for statistical self-similarity is present in certain ‘aspects’ of the traffic, the multifractal scaling behavior is much more convincing. Furthermore, crucial LAN specific characteristics of data traffic are revealed by the multifractal analysis (MA) only. TCP traffic at Berkeley and at CNET, e.g., looks entirely different from a multifractal point of view while showing about the same self-similarity parameter  $H$ . As a further example, MA suggests that Lévy stable motion is in certain situations a more accurate model than FBM. In conclusion, to consider traffic traces as multifractal random measures rather than as (monofractal) self-similar processes is not only more natural but has also various numerical advantages. A novel approach to queueing supports this conclusion.

## 1 Introduction

”Fractal” analysis of computer network traffic has recently been the subject of various studies [LTWW, N1, N2, TTW1, TTW2]. Most of the effort has been focused on measuring and modeling a possible *long range dependence* in the data. This was motivated by a thorough experimental study [LTWW] providing strong evidence for the presence of long range dependence in real data traffic. Such a property would have important consequences in many area such as queueing theory [N1, N2] or network design.

However, long range dependence is only one feature of a ”fractal” behavior. In this work, rather different properties are under study which are conveniently described using *multifractal analysis* (MA). Very roughly speaking, while previous studies tried to investigate the *low frequency* content of the signal, the *high frequencies* are the part of interest here. The motivation for studying these high frequencies is twofold : first, in applications such as traffic control, attempting to understanding *large rapid variations* may prove more crucial than looking for long term correlations. Second, to find or disprove a relation between the local behavior of the signal (revealed by a multifractal analysis) and the apparent long range dependence (revealed by former studies) is of essential interest. Indeed, for some simple fractal models such as *fractional Brownian motion* (proposed by several authors for traffic modeling [LTWW, N1, N2]), the exponent governing the local singular behavior is identically equal to the Hurst exponent  $H$  ruling the long range dependence. For general processes, such as stable Lévy motion, the local singular behavior depends on time and is best described by the multifractal spectrum of singularity exponents.

Multifractal analysis goes one step further when suggesting that traffic traces should not be considered as self-similar processes but rather as random multiplicative measures. As will be explained, an essential issue is whether or not the increment process should be centered for numerical analysis. MA may, thus, shed new light on the adequacy of previously proposed models by looking at very different properties of them, and help to clarify this rapidly evolving topic.

Section 2 features an introduction to multifractal measures, a motivation for their use in traffic modeling, and a comparison of the multifractal and statistical methods of scaling. In Section 3 the numerical analysis of several real traffic traces is presented, addressing in particular quality and significance of the results in a comparison of the multifractal and the statistical approach. The multifractal spectra obtained allow to draw conclusions of a general kind.

## 2 Multifractal Analysis

It is well known that the geometrical complexity of a ‘fractal’ set may be described, at least in a global way, by giving its dimension [F]. In order to provide more detailed

information, multifractal analysis is concerned with describing the local singular behavior of measures, distributions, and functions [M1, AP, GP, HJKPS].

This may be done in geometrical terms using the notion of fractal dimensions [AP, F], an approach which will not further be mentioned here. Alternatively, and more interesting from point of view of applications, one may follow the method of coarse graining and aim for a statistical description which is intimately related to large deviation principles (LDP) as is explained below [EM, R, LV].

## 2.1 Multifractal measures

Assume that a measure  $\mu$  supported on the unit interval  $[0, 1]$  is given and consider the random variables  $Y_n = \log \mu(I_K^{(n)})$  where  $I_k^{(n)} := [k2^{-n}, (k+1)2^{-n}]$  and  $K$  is a random number from  $\{0, \dots, 2^n - 1\}$  with uniform distribution  $P_n$ . If the rate function (elsewhere also called ‘partition function’ or ‘free energy’ [GP, HJKPS, R, M1])

$$\tau(q) := -1 + \lim_{n \rightarrow \infty} \frac{-1}{n} \log_2 \mathbb{E}_n[\exp(qY_n)] = \lim_{n \rightarrow \infty} \frac{-1}{n} \log_2 \sum_{k=1}^{2^n} \mu(I_k^{(n)})^q \quad (1)$$

exists and is differentiable on  $\mathbb{R}$ , then a simple application of the Gärtner-Ellis theorem on Large Deviations [Ell, R] shows that the double limit

$$f_G(\alpha) := \lim_{\varepsilon \rightarrow 0} \lim_{n \rightarrow \infty} \frac{1}{n} \log_2 2^n P_n[\alpha(I_K^{(n)}) \in (\alpha - \varepsilon, \alpha + \varepsilon)] \quad (2)$$

with

$$\alpha(I_K^{(n)}) := \frac{-1}{n \log 2} Y_n = \frac{\log \mu(I_K^{(n)})}{\log |I_K^{(n)}|}.$$

exists, and, moreover

$$f_G(\alpha) = f_L(\alpha) := \tau^*(\alpha) := \inf_{q \in \mathbb{R}} (q\alpha - \tau(q)). \quad (3)$$

The function  $f_G$  captures quantitatively the deviation of the so-called *coarse Hölder exponent*  $\alpha(I_K^{(n)})$  from its expected value. It has been termed *coarse grain (multifractal) spectrum*. Due to its importance the Legendre transform of  $\tau(q)$ , here denoted by  $f_L$ , is often referred to as *Legendre (multifractal) spectrum*.

The equation (3) is usually referred to as the *multifractal formalism*. Considerable work has been dedicated to the task of establishing it under as weak assumptions as possible. If it holds, the somewhat involved but rich  $f_G$  may be estimated through the more robust and simpler  $f_L$ .

There are convincing examples where  $f_G$  is not concave, hence different from  $f_L$ , but in all generality a weak form of (3) is true [R]:

$$\tau(q) = \inf_{\alpha} (q\alpha - f_G(\alpha)). \quad (4)$$

In other words,  $f_L$  is always the concave hull of  $f_G$ . Consequently,

$$f_L(\alpha) \geq f_G(\alpha). \quad (5)$$

By the way, note that  $f_G(\alpha)$  and  $f_L(\alpha)$  are always positive in the setting of (2) since  $2^n P_n[A]$  is simply the number of integers in  $A$ . The typical shape of  $f_L$  is a  $\cap$ .

A class of measures which satisfy the LDP (2) are the Binomial distributions which are generated by a Bernoulli trial. Fix two positive numbers  $m_0, m_1$  with  $m_0 + m_1 = 1$  and represent points  $x \in [0, 1]$  by their dyadic expansion  $x = (0.\sigma_1\sigma_2\dots)_2$ . The Binomial distributions is then defined by picking  $x$  randomly such that  $P[\sigma_k = i] = m_i$  ( $i = 0, 1$ ) independently of  $k$ . In this simple case,  $\mu(I_K^{(n)}) = m_{\sigma_1} \cdot \dots \cdot m_{\sigma_n}$ , whence  $\alpha(I_K^{(n)}) = -\frac{1}{n} \sum_{l=1}^n \log_2 m_{\sigma_l}$ , where the sequence  $\sigma_l$  is uniquely determined by  $K$  via the condition  $0.\sigma_1\sigma_2\dots\sigma_n \in I_K^{(n)}$ . The LLN implies that  $\alpha(I_K^{(n)}) \rightarrow \alpha_0 := \mathbb{E}_{\lambda}[-\log_2 m_{\sigma_1}] = -\frac{1}{2} \log_2 m_0 m_1$  ( $n \rightarrow \infty$ ) almost surely. Besides  $\alpha_0$ , other coarse Hölder exponents  $\alpha(I_k^{(n)})$  will be observed such as  $\alpha_{\min} = \log m_0 / \log(1/2)$  and  $\alpha_{\max} = \log m_1 / \log(1/2)$ <sup>1</sup>, though more and more rarely as  $n \rightarrow \infty$ . More precisely, one finds

$$\tau(q) = -\log_2 (m_0^q + m_1^q), \quad (6)$$

which yields a  $\cap$ -shaped spectrum  $f_L$  with maximum  $f_L(\alpha_0) = 1$ , and which is positive in  $]\alpha_{\min}, \alpha_{\max}[$ , vanishes in  $\alpha_{\min}$  and  $\alpha_{\max}$  and is trivial, i.e.  $-\infty$  outside this interval.

The parameter  $\alpha$  quantifies the degree of regularity in a point  $x$ : loosely speaking, the measure of an interval  $[x, x + \Delta x]$  — in applications usually the number of events occurring in this interval — behaves as  $(\Delta x)^\alpha$ . Consequently,  $\alpha < 1$  indicates a burst of events around  $x$  ‘on all levels’ (bursts of bursts), while  $\alpha > 1$  is found in regions where events occur sparsely. All this information is captured in  $f_G$ , and, provided it exists and is differentiable, also in the rate function  $\tau(q)$ .

As an important generalization let us introduce the random binomial measures. Fix the distributions of 2 random variables  $M_0$  and  $M_1$  such that  $\mathbb{E}_{\omega}[M_0 + M_1] = 1$ . Then, define a random distribution  $\mu$  by picking  $x = .\sigma_1\sigma_2\dots \in [0, 1]$  in a ‘doubly random way’, i.e. such that for a given realization  $\mu(\omega)$  the  $(\mu)$ -probability for  $\sigma_k = i$  equals  $M_{\sigma_1\dots\sigma_{k-1}i}$ , and such that  $M_{\sigma_1\dots\sigma_{k-1}0}$  are i.i.d.  $(\omega)$ -random variables with law  $M_0$ , and similar for  $M_{\sigma_1\dots\sigma_{k-1}1}$ . In other words, the  $\mu$ -measure of a fixed interval  $I_k^{(n)}$  is a  $\omega$ -random variable and equals  $\mu(I_k^{(n)}) = M_{\sigma_1} \cdot M_{\sigma_1\sigma_2} \cdot \dots \cdot M_{\sigma_1\dots\sigma_n}$  where  $.\sigma_1\dots\sigma_n$  is the dyadic representation of  $k2^{-n}$ . This way of redistributing mass by iterative bisection independently and identically in each step of the construction could fairly be called *multifractal stationarity*. As a sum of

<sup>1</sup>Without loss of generality  $m_0 \geq m_1$  was assumed.

i.i.d. random variables,  $\log \mu(I_k^{(n)})$  is approximately Gaussian, if properly normalized and provided that the  $\log M_i$  have finite second moments. A ‘multifractal process’ has, thus, approximately log-normal marginals.

For these *random multifractals*, the LDP holds with probability space  $\{0, \dots, 2^{n-1}\} \times \Omega$  and

$$\tau(q) = -\log_2 \mathbb{E}_\omega[M_0^q + M_1^q].$$

While  $f_L(\alpha)$  is always positive in the deterministic case due to (5), negative values may occur with random measures. If so, the probability of observing  $\alpha$  decreases too fast and the factor  $2^n$  – used in (2) in order to account for the number of intervals available at resolution  $n$  – is not increasing sufficiently fast. The corresponding Hölder exponents are, thus, only observed when oversampling the process at least  $2^{-nf_L(\alpha)}$  times [M2, LR]. Then, at least in the average, one of the  $2^{n(1-f_L(\alpha))}$  intervals of size  $2^{-n}$  now available should show the Hölder exponent  $\alpha$ .

## 2.2 Motivation

Before going further into the details of the analysis performed we would like to motivate the multifractal approach in the study of data traffic.

The first argument is a visual one. In Fig. 1 a *self-similar random measure* as above is compared with a trace of real data traffic. The striking resemblance makes multifractals a natural candidate for data traffic modeling.

Second, the increments of self-similar processes (used so far as fractal models of data traffic) are necessarily of zero mean while multifractals, being measures, possess only positive increments. In addition, the increments of multiplicative measures are approximately log-normal — and not Gaussian as the increments of FBM — in agreement with observations on real data traces [P].

Third, it is natural to consider *invariant* random distributions, such as self-similar random multifractals, as models of traces of data traffic as the following novel approach to queueing suggests. To start, consider the more general random *multiplicative* measures  $\mu$  defined by

$$\mu(E) := \lim_{n \rightarrow \infty} \int_E Q_1(t) \cdot \dots \cdot Q_n(t) dt, \quad (7)$$

where the  $Q_n$  are positive random functions with  $\mathbb{E}Q_n(t) = 1$  for all  $t$ . (For the random binomial measure above, the  $Q_n$  are piecewise constant:  $Q_n(t) = 2^n M_{\sigma_1 \dots \sigma_k}$  in  $I_k^{(n)}$ .)

Intuitively, one thinks of the limiting product of the  $Q_n$  as the rate of oncoming traffic at a gateway and of  $\mu(E)$  as the total traffic load arrived in time interval  $E$ . Thereby, it is essential to note that the limit of the  $Q_n$  is not a function, but a distribution. Thus,

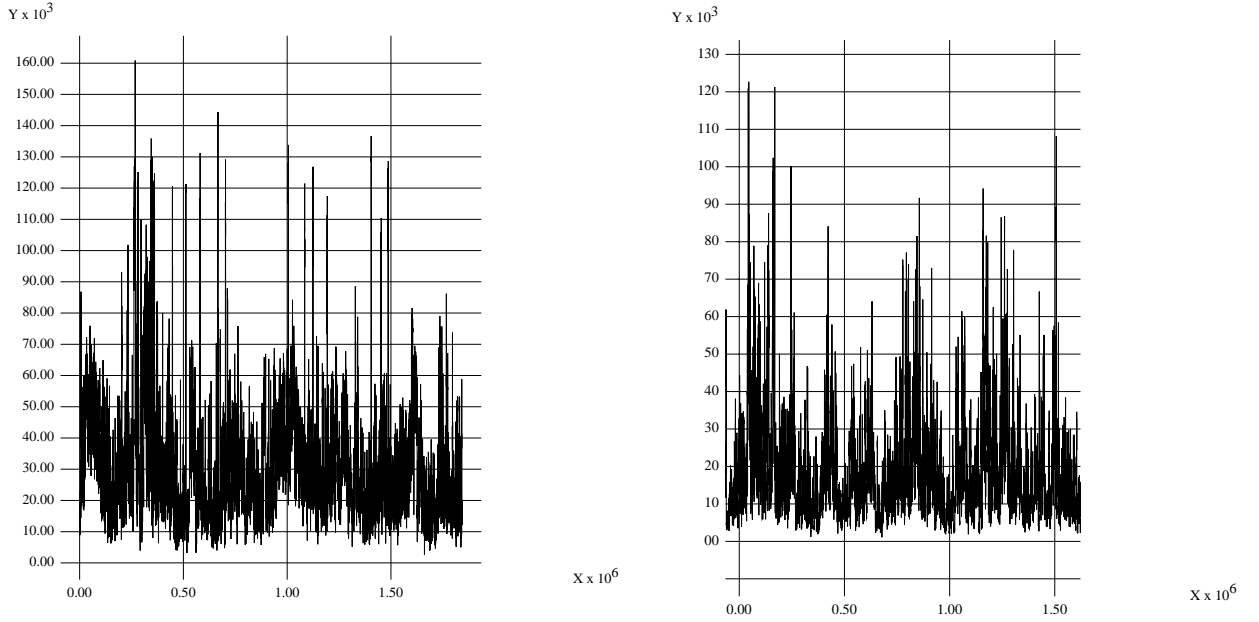


Figure 1: Traffic observed at the gateway of Berkeley and the measure obtained by a randomized version of the Binomial measure.

the intuition is rigorously correct only in terms of average arrival rates in ‘short time intervals’:  $\mu(I_k^{(n)})/|I_k^{(n)}|$ .

With this idea in mind of modeling traffic in a multiplicative rather than an additive way, the passing of a trace through a server queue is modeled simply as a change of this rate:

$$Q(t) \simeq \lim_{I_k^{(n)} \searrow t} \mu'(I_k^{(n)})/\mu(I_k^{(n)}).$$

Stability requires that  $\mathbb{E}Q(t) = 1$ . In more precise terms, let us model the passing of a traffic stream through a server queue by a random multiplier function  $Q$ , i.e.  $Q(t) \geq 0$  and  $\mathbb{E}Q(t) = 1$ , in the following way:

$$\mu(E) := \int_E Q_1(t) \cdot \dots \cdot Q_n(t) dt \mapsto \mu'(E) := \int_E Q(t) \cdot Q_1(t) \cdot \dots \cdot Q_n(t) dt. \quad (8)$$

In other words,  $Q(t)$  models the bit-rate of a traffic stream with constant rate after it has passed through the server queue. In the typical case where  $Q$  will be a piecewise constant function it is possible to write again more explicitly

$$\mu'(E) = \sum_{i=0}^M Q^i \int_{T_i}^{T_{i+1}} d\mu$$

where the  $Q^i$  are the random values which  $Q$  takes on the random subintervals  $[T_i, T_{i+1}]$  of  $E$ .

The last ingredient to this approach is the assumption that a WAN consists of an infinity of server queues that can be modeled by random multipliers as in (8). What remains is a simple fix-point argument: A data stream may ideally be considered as a uniformly distributed sequence of bytes at the moment when it starts being transferred (thus modeled by the measure  $dt$ ). Passing through an ‘infinite’ number of server queues it will eventually become statistically invariant under the operation  $\mu \mapsto \mu'$  (8). Hence, it makes sense to model traffic traces by the fix-point (7).

In conclusion, multiplicative random measures, should be considered as valuable models of TCP traffic.

To end, let us recall that computing multifractal spectra will prove useful in the following sense: provided that the scaling is good over many orders of magnitude (which is indeed the case) estimating spectra on coarse resolution will allow to conclude on the statistical behavior on high resolution, i.e. in short time intervals.

### 2.3 Multifractal scaling

Based on the general remarks in Subsection 2.1 the notions of multifractal and statistical scaling of moments are now made precise. It will be argued that the multifractal method is more natural when positive data such as traffic data is to be investigated since there is no need to center the data before analyzing. A further comparison of the two approaches is postponed to Subsection 3.3 where the necessary data analysis is available.

Let us consider a sequence of positive numbers  $(Z_i)_{i=1}^N$  which may represent any interesting information on the traffic load passing through a gateway. (In Section 3 this letter will be reserved for one particular data). Among many other ways of analyzing one may interpret the data as a) a sampling of a random measure where  $Z_i / \sum_i Z_i$  is the probability for a byte to arrive at time  $t_i$ , or b) as a path of a stochastic process.

In the former case, a multifractal analysis is in order. In the latter case, it has been widely agreed [LTWW, N1, N2] that the most important fractal statistical parameter to be estimated is the degree of *long range dependence* (LRD), usually measured through the *Hurst exponent*  $H$ . Among the various methods of estimating  $H$  [TTW1, TTW2] the method of moments comes closest to the multifractal approach.

First, let us consider the data  $(Z_i)_{i=1}^N$  as a sampling of a measure  $\mu$  on  $[0, 1]$  at scale  $\delta = 1/N$  and define the *partition sum* through

$$S_m^Z(q) := \sum_{k=1}^{N/m} (\bar{Z}_k^{(m)})^q,$$

where

$$\overline{Z}_k^{(m)} := \sum_{l=1}^m Z_{(k-1)m+l}$$

provides a sampling of  $\mu$  at scale  $\delta_m = m/N$ . If  $\log S_m^Z(q)$  is in good approximation linearly depending on  $\log m$ , we say that the data exhibits *multifractal scaling*, in short:  $Z_i$  is a multifractal. Referring to (1) the slope of the linear law, usually obtained by least square fitting, is denoted by  $\tau^Z(q)$ , or shortly  $\tau(q)$ :

$$\log S_m^Z(q) \simeq \tau^Z(q) \cdot \log m + \text{const.} \quad (9)$$

In order to visualize the quality of a linear approximation of the graph of  $\log_2 S_m^Z(q)$  versus  $\log_2 m$  it is useful to look at the piecewise increments of  $\log_2 S_m^Z(q)$ , i.e.

$$\tau_m^Z(q) := \tau(Z, m, q) := \log_2 S_{2m}^Z(q) - \log_2 S_m^Z(q) \quad (10)$$

as a function of  $\log_2 m$ . If  $\tau_m(q) \simeq \tau(q)$  independently of  $m$  then (9) holds in good approximation. In praxis, however, one computes  $\tau(q)$  through a least square fitting rather than through averaging  $\tau_m(q)$ . The behavior of the latter, though, can be used to determine the *scaling region*, i.e. the range of  $m$  in which the fitting is performed.

As  $\tau(q)$  has a slope which varies often only little, typically in the range  $[1/2, 2]$ , its plot may appear to be almost linear to the naked eye. Therefore, displaying its Legendre transform  $f_L$  is more informative. Moreover, the interpretation in terms of burstiness and regularity comes more natural with  $f_L$  (compare (2)). Recall, that  $f_L$  may show **negative** values due to under-sampling. In other words,  $f_L(\alpha) < 0$  corresponds to very rare Hölder exponents as explained in Subsection 2.1.

## 2.4 Statistical scaling

The statistical approach of interest here relies on the notion of *self-similar processes*. Consider a process  $Y_i$  with stationary increments  $X_i = Y_i - Y_{i-1}$ . Assume that  $Y_i$  is  $H$ -self-similar, i.e.

$$Y_{mi} \stackrel{d}{=} m^H Y_i.$$

Let

$$X_k^{(m)} = 1/m \sum_{l=1}^m X_{(k-1)m+l} = 1/m \overline{X}_k^{(m)}.$$

Then,

$$X_k \stackrel{d}{=} m^{1-H} X_k^{(m)}. \quad (11)$$

As was proposed by Taqqu, Teverovsky & Willinger recently [TTW2], a test of self-similarity could be performed through the behavior of the absolute moments. An estima-

tor of  $\mathbb{E}|X^{(m)}|^q$  would be

$$\hat{\mathbb{E}}|X^{(m)}|^q := \frac{1}{N/m} \sum_{k=1}^{N/m} |X_k^{(m)}|^q.$$

In analogy to multifractal analysis let us consider rather

$$S_m^X(q) := \sum_{k=1}^{N/m} |\bar{X}_k^{(m)}|^q = m^{q-1} N \cdot \hat{\mathbb{E}}|X^{(m)}|^q.$$

If  $X_i$  is self-similar in the sense of (11) one finds

$$\log S_m^X(q) \simeq \gamma(q) \cdot \log m + \text{const.} \quad (12)$$

Moreover,  $\gamma(q)$  is then linear in  $q$ :

$$\gamma(q) = qH - 1.$$

Thus, Taqqu et al. [TTW2] propose a test of self-similarity which translates into the present setting as: Determine whether there is  $\gamma$  such that (12) holds approximately. If  $\gamma$  depends linearly in  $q$  then the data may be called self-similar in the sense of (11).

It is worth noting, first of all, that (11) implies together with stationarity that

$$\text{either } \mathbb{E}X = 0, \quad \text{or } \mathbb{E}X = \pm\infty, \quad \text{or } H = 1.$$

But  $H = 1$  implies that  $Y_t = t \cdot Y_1$  almost surely. In other words, the concept of statistical self-similarity (12) makes sense only after centering the data, i.e. in this context when setting

$$X_i := Z_i - \hat{\mathbb{E}}Z = Z_i - 1/N \sum_{i=1}^N Z_i.$$

In Section 3 the corresponding scaling exponent (12) will be denoted by  $\gamma^Z$  in order to refer to the original non-centered data.

Multifractal analysis as presented here, on the other hand, is perfectly fitted to positive data such as data traffic measurements. Further comparison of the multifractal and the statistical approach is postponed to Subsection 3.3. Here, it should be added that a multifractal analysis of processes with arbitrary increments is being developed using wavelets.

### 3 Numerical analysis of the TCP traffic

Most of the numerical results presented here concern  $f_L$  since it would be beyond the scope of this paper to indulge in the rather involved estimation techniques of  $f_G$ . Nevertheless,

it is notable that rule ‘ $f_L$  is the concave hull of  $f_G$ ’ has always been found to be met to a satisfactory degree, which speaks for the accuracy of the estimation.

The traces analyzed in this study are records of TCP–data traffic collected at the gateway of a LAN. The first trace which will be reported on extensively corresponds to two hours at Berkeley. Further traces are records of eight hours at CNET labs on different days. They have been used for comparison and for studies of stationarity. All traces contain about  $2^{21}$  observations, consisting of the arrival time  $T_i$  of the packet number  $i$ , the size  $Z_i$  of the packet in number of bytes, as well as information regarding sender and recipient.

This information allowed to distinguish between the traffic entering the LAN, called *incoming*, and the traffic leaving the LAN, called *outgoing*. It should be stressed here that the incoming traffic is, therefore, generated by a WAN traffic, thus (WAN-LAN), while the outgoing one is produced by a LAN traffic, thus (LAN-WAN). Both traffic streams, however, have to pass through the same gateway, producing the measured traffic load  $Z_i$ . This is what will be addressed with the term ‘traffic’, resp. with *combined traffic* if confusion is possible. As a general remark the readers attention is drawn to a technical report [RL1], available on the WWW, which contains further details on this study.

### 3.1 Trace recorded at Berkeley

**Notation:** From the data contained in the traces one can extract the following measures of the traffic flow: the ‘number of bytes of packet’  $Z_i$ , the ‘inter-arrival time between packets’  $T_i$ , the ‘number of bytes arriving per time’  $B_k$ , and ‘number of packets arriving per time’  $P_k$ . These will be addressed as *aspects* of the traffic. The corresponding multifractal (9), resp. statistical (12) scaling exponents will be denoted by  $\tau^Z, \gamma^Z, \dots, \tau^P$  and  $\gamma^P$ , respectively.

#### 3.1.1 Bytes per packet

The first aspect investigated was  $Z_i$ , i.e. the ‘bytes per packet’. Not only is this aspect the most easily accessible, it poses also no problems when separating incoming and outgoing traffic.

At first sight, one would not expect an interesting behavior, since TCP packets are mostly either very small (ACK, NACK) or very large. This reasoning, however, considers only the histogram at the finest time scale. Apparently, the aspect  $Z_i$  reveals essential characteristics of the traffic. In particular, there is excellent multifractal scaling though there is only little variability in the data  $Z_i$ , meaning that there are clusters of very large (small) packets, clusters of clusters, and so on. In other words, no ‘averaging’ takes place. To the contrary, the multifractal properties of  $Z_i$  allow to clearly distinguish between outgoing

and incoming traffic and demonstrate the striking difference between traffic generated at the University of Berkeley versus the one produces at the research laboratories of CNET.

Let us report on the multifractal scaling first. Excellent multifractal scaling of  $S_m^Z(q)$  was found for all  $q$  when choosing  $m = 25, 50, 100, \dots, 1600$  (not displayed) as well as when taking  $m = 1, 2, 4, \dots, 2^{19}$  (see Fig. 2). The linear behavior is of exceptional quality. The  $\tau^Z(q)$  obtained from a least square fitting of  $\log S_m^Z(q)$  against  $\log m$  looks almost linear to the naked eye why it is preferable to display the Legendre spectrum  $f_L = \tau^*$ .

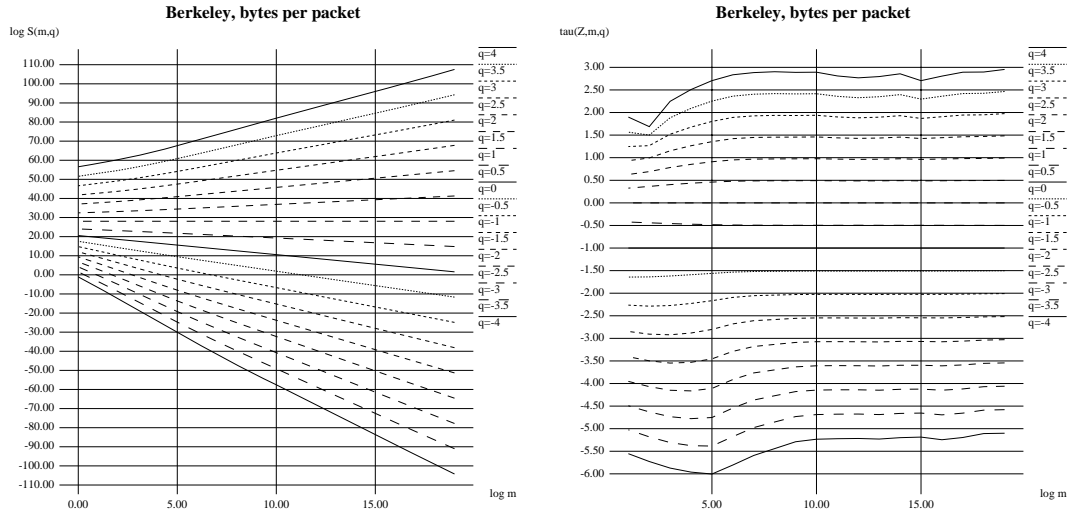


Figure 2: The scaling behavior of  $Z_i$  (bytes per packet) for the (combined) traffic observed at Berkeley demonstrated in log-log plots of  $S_m^Z(q)$  against  $m$ , where from top to bottom  $q$  runs through 4, 3.5, 3,  $\dots$ , -3.5, -4. For a better visualization of the quality of a linear approximation of these plots, the piecewise increments (10) are shown on the right.

Several arguments speak for the reliability of the numerical estimation of  $\tau$ . There are certainly the excellent correlation coefficients of the least square fit as is evident from Fig. 2. A strong advocate is also the excellent agreement with the ‘weak multifractal formalism’ (4), i.e.  $f_L$  is a convincing concave hull to  $f_G$ . Fig. 3 displays estimates of  $f_G$  computed via a ‘double kernel method’ [RL1] at various levels of aggregation  $n$  with an ‘optimal’  $\varepsilon = \varepsilon(n)$ . For comparison note that  $n$  of (2) and  $m$  of (9) are related by  $m = N2^{-n}$  where  $N = 2^{21}$  is the number of records. Finally, the shapes of various  $f_L$  have definite characteristic features. They are, e.g. different for incoming and outgoing traffic throughout the data considered here (see below) and they confirm certain theoretical predictions when comparing different aspects (see Fig. 6 and 3.1.3).

Unfortunately, it is beyond the scope of this paper to report in detail on  $f_G$ . It is worthwhile, though, to mention the non concave part in the spectrum of  $Z$  (see Fig. 3). The ‘wiggle’ of  $f_G$  suggests that the traffic has two ‘phases’, in analogy with multifractals with similar spectra [R, Ex. 2]. The first and immediate guess saw these phases in the

incoming and the outgoing traffic and is responsible for their being consequently analyzed separately. The surprise came with the news that the outgoing traffic showed indeed only one bump as expected, but the incoming traffic displayed now two almost entirely separated bumps. In conclusion, the incoming traffic most likely consists of two ‘phases’ which are widely independent, i.e. which occur at ‘well separated’ times, one being more bursty and occurring more rarely, the other one being more regular and almost always present. These observations have been confirmed by later studies [NM]. (Incoming and outgoing traffic are not independent in this sense which is why the two bumps of the spectrum of the incoming traffic get washed out when the two streams are merged to the combined traffic.)

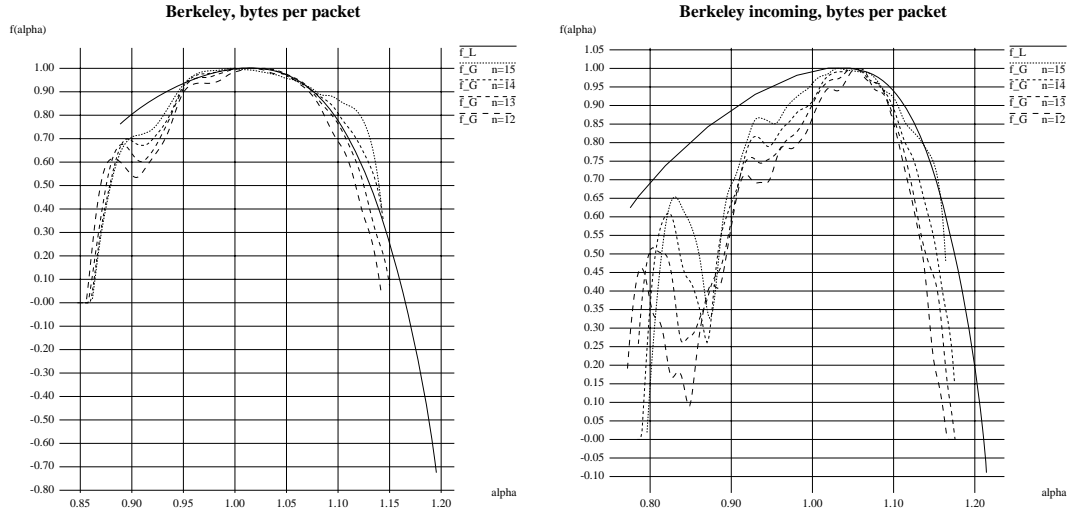


Figure 3: The Legendre spectrum  $f_L$  is a convincing concave hull to the coarse grain spectrum  $f_G$ , as predicted by the ‘weak multifractal formalism’ (4). The apparent non concave shape of  $f_G$  is produced uniquely by the incoming component of the traffic. The two clearly separated bumps suggest that the incoming traffic consists of two independent ‘phases’.

With the statistical approach the scaling behavior is less favorable. For the centered data  $X_i := Z_i - \hat{\mathbb{E}}Z$  the scaling behavior of the partition sum  $S_m^X(q)$  was acceptable only for *positive*  $q$  (see Fig. 4). For negative  $q$  the log–log plots were far from being linear, obviously due to very small values  $|X_k^{(m)}| \ll 1$  produced when centering the data. From the point of view of scaling, thus, it can be regarded as a disadvantage having to center the data in the ‘statistical scaling approach’.

But the estimates  $\gamma_m^Z(q)$  suffer from high variability even in the positive  $q$  range. The estimation of  $H$  in particular depends highly on the choice of the scaling region and cannot be called robust (Subsection 3.3). Nevertheless, the scaling function  $\gamma^Z(q)$  is fairly linear for  $q \geq 1$ . This linearity corresponds to a Legendre transform  $\gamma^*$  which ‘stops’ at the point with slope  $q = 1$  (see Fig. 5). The decreasing part, though displayed, is not

reliable since there was poor scaling for negative  $q$  (see Fig. 4). Most importantly, with the centered data  $X_i = Z_i - \hat{\mathbb{E}}Z$  a less significant difference could be observed between incoming and outgoing traffic, i.e. the reliable increasing part of the  $\gamma^*$ -spectra (Fig. 5) are note as clearly distinguishable as the ones of the non-centered data (Fig. 6).

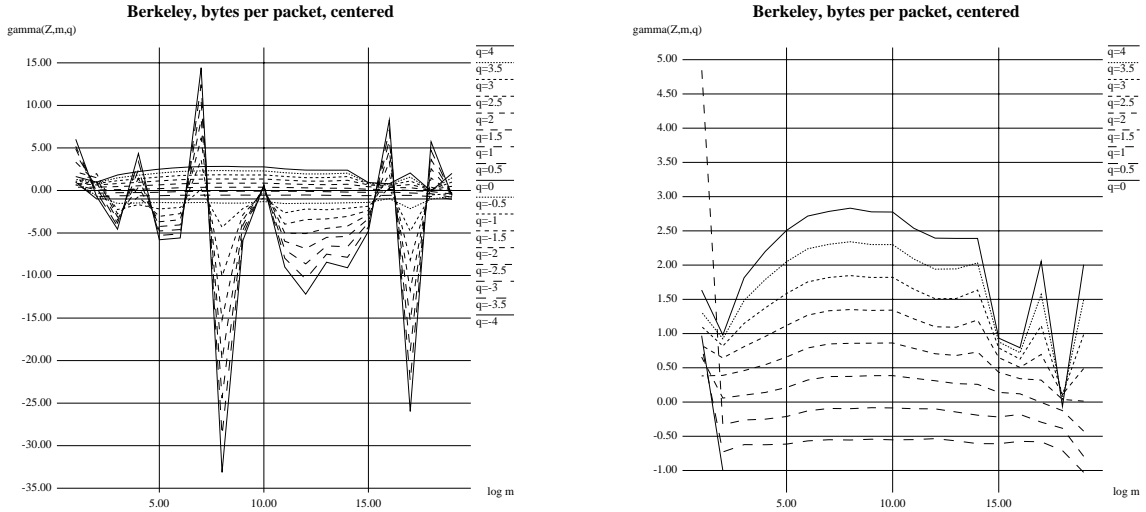


Figure 4: Scaling behavior of the centered data  $X_i = Z_i - \hat{\mathbb{E}}Z$  for the same source as in Fig. 2, demonstrated in plots of the piecewise increments  $\gamma_m^Z(q) = \gamma(Z, m, q) = \log_2 S_{2m}^Z(q) - \log_2 S_m^Z(q)$  (compare (10)). It is clear that one cannot talk of scaling for negative  $q$ . But also for positive  $q$  one finds high variations of up to 100% (see close up on the right). This lack of robustness has drastic consequences which are discussed in Subsection 3.3, in particular in Table 2.

### 3.1.2 Inter-arrival times (Time per packets)

The next simple aspect from the point of view of an analysis is ‘time per packet’. When separating incoming and outgoing traffic the absolute arriving times were kept rather than the inter-arrival times when separating incoming and outgoing traffic. This takes into account the mutual influence of the two data streams as it is observed at the gateway and is the natural way of proceeding since there are also other protocols apart from TCP passing through the same gateway, making a clear distinction impossible and, in fact, undesired.

All of what has been said about the quality of the multifractal and the statistical scaling behavior for the ‘bytes per packets’ applies here too. See Fig. 6 for the multifractal spectra. It is notable, that there is no significant difference between incoming and outgoing traffic when analyzing the inter-arrival time process from the statistical point of view, which seems to be common practice so far (see Fig. 5, Subsection 3.3, Table 2).

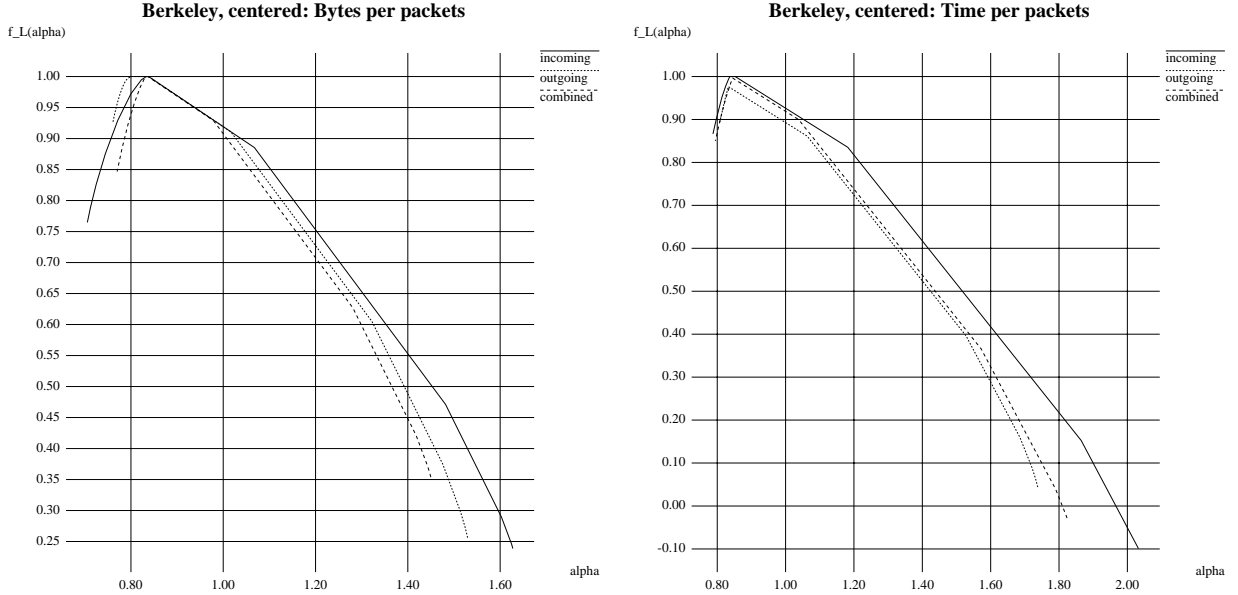


Figure 5: The Legendre transform of  $\gamma^Z(q)$  and  $\gamma^T(q)$  which were obtained by least square fitting of Fig. 4 for  $\gamma^Z(q)$  and the corresponding data for  $\gamma^T(q)$  in the scaling region  $m = 2^4, \dots, 2^9$ . The complete curves have been calculated despite of poor scaling in the range  $q < 0$  which corresponds to the decreasing part of the spectra. The difference between incoming and outgoing traffic shows only with the aspect ‘bytes per packets’. From an analysis of the inter-arrival times, the two traffic look alike. In particular, the LRD parameter  $H$  (peak of the spectra) lie in the range  $[\.832, \.845]$  for  $T_i$ . In this context it is important to mention, though, that the spectra show a clear edge at the maximum. This is equivalent to saying that  $\gamma(q)$  is linear for a considerable range of  $q$  which indicates statistical self-similarity (12).

A tentative explanation for this insensitivity may be found in the fact that data transfer by TCP requires acknowledgment so that incoming as well as outgoing inter-arrival times depend mostly on the round trip time of a connection. A measurement of  $H$  will capture the LRD, i.e. the second order statistics. A multifractal analysis will in addition to this display information about the negative moments in its decreasing part. Thus, it captures also the burstiness of the inverse process  $P$  which contains more explicit information about the traffic load (Fig. 6). But the inversion formula (13) holds for measures only, and not for general processes.

### 3.1.3 Aspects with respect to time

From point of view of an application in traffic modeling the most interesting aspect are certainly the ones with respect to ‘time’. When cumulating data into time-intervals of equal length one has to be aware, though, that additional information may be created.

As the various methods all yield the same  $\tau$  [RL1] the multifractal behavior may be considered as being established.

The three methods of cumulating are the following, all based on new time instances  $t_k = k \cdot \delta t$  with a fixed time interval  $\delta t$ .

- Compute the ‘number’ of packets  $P_k$  arriving in the artificial time interval  $I_k := [t_k, t_{k+1}]$ , accounting for each effective arrival interval  $[T_i, T_{i+1}]$  according to its ‘time spent in  $I_k$ ’:

$$P_k = P_k(\delta t) = \sum_i \frac{|[T_i, T_{i+1}] \cap I_k|}{|[T_i, T_{i+1}]|}$$

where  $|\cdot|$  denotes the length of an interval. Similarly, the ‘number’ of bytes  $B_k$  ‘arriving’ in  $I_k$  is

$$B_k = B_k(\delta t) = \sum_i Z_i \cdot \frac{|[T_i, T_{i+1}] \cap I_k|}{|[T_i, T_{i+1}]|}.$$

With this method, artificial information has been created.

- Approximate uniform inter-arrival times  $\delta t$  as closely as possible by choosing actual time instances  $T_{l(k)}$  such that

$$T_{l(k)} \leq T_{l(k-1)} + \delta t < T_{l(k)+1}.$$

For this procedure to make sense, we need  $\delta t \geq T_{i+1} - T_i$  for all  $i$ . Now, take  $P_k^*(\delta t) := l(k+1) - l(k)$  and, consequently,

$$B_k^* = B_k^*(\delta t) = \sum_{i=l(k)}^{l(k+1)-1} Z_i.$$

No additional information has been created for the price of having non-uniform time intervals. In order to switch from time scale  $\delta t$  to  $2 \cdot \delta t$ ,  $4 \cdot \delta t$ ,  $8 \cdot \delta t$  etc. one may

- repeat the procedure with time step  $2\delta t$ , i.e. consider  $P_k^*(2 \cdot \delta t)$ ,  $P_k^*(4 \cdot \delta t)$ , etc. and similarly for  $B^*$ ,
- or simply cumulate recursively, i.e. consider  $P_k^{**}(\delta t) := P_k^*(\delta t)$ ,  $P_k^{**}(2^{l+1} \cdot \delta t) := P_{2^{k-1}}^{**}(2^l \delta t) + P_{2^k}^{**}(2^l \delta t)$ , and similarly for  $B^{**}$ .

It is clear that the computation is faster in the second case but that the approximation is better in the first case. The piecewise increments  $\tau_m$  showed no significant difference for the three methods, leading to virtually the same estimates of  $\tau(q)$  [RL1].

Of particular interest is the aspect ‘packets per time’  $P_k$  since it is ‘inverse’ to the aspect ‘time per packet’  $T_i$ . Theory [MR, RM] says that the spectra of inverse measures are related by the formula

$$f^T(\alpha) = \alpha f^P(1/\alpha), \quad (13)$$

resp.

$$\tau^T = -q^P \quad \text{and} \quad \tau^P = -q^T.$$

Note, that the transformation  $(\alpha, f) \mapsto (1/\alpha, 1/\alpha \cdot f)$  exchanges the bisector of the axes  $f = \alpha$  with the horizontal line  $f \equiv 1$ , the two typical touching lines of a spectrum. Whence, the ‘symmetry’ of the spectra  $f_L^T$  and  $f_L^P$  which is clearly visible in Fig. 6.

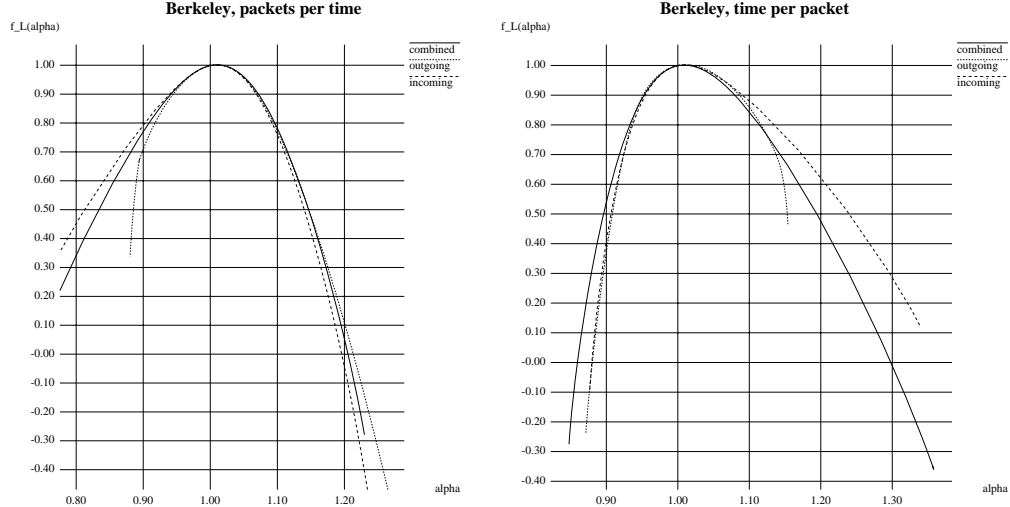


Figure 6: At Berkeley, the incoming traffic shows spectra  $f_L$  which are characteristically different from the the ones of the outgoing traffic and the combined traffic. This becomes apparent when studying any aspect. Of special interest are the aspects  $P_k$  and  $T_i$  (‘packets per time’ and ‘time per packet’) due to their intrinsic symmetry. These aspects provide samplings of measures which are *inverse* to each other [MR, RM]. Theory says that the spectra of inverse measures must be related through the formula  $f_L^P(\alpha) = \alpha f_L^T(1/\alpha)$ . The estimates, which were obtained from  $\tau(q)$  for  $q = -40, -39, \dots, 40$ , show a convincing match.

Several remarks are in order.

- First, the fact that the predicted symmetry between  $f_L^T$  and  $f_L^P$  holds with high accuracy proves that these spectra contain significant and correct information.
- Second and most importantly, it should be stressed that the main difference between the observed outgoing and incoming traffic remains hidden to an analysis based on statistical scaling analysis of the inter-arrival times  $T_i$ , since this difference manifests itself in the part of the spectrum corresponding to *negative*  $q$ . There, the scaling of centered data is poor (see Fig. 4 and 8) and the resulting partition function is linear and contains no information (see Fig. 5).
- Finally, all aspects reflecting the ‘traffic load’ ( $Z_i$ ,  $P_k$  and  $B_k$ ) show that the outgoing traffic observed at Berkeley is clearly more regular and less bursty than the incoming traffic [RL1].

### 3.2 Traffic at CNET Labs

An analysis of traffic at the LAN at CNET Laboratories showed again excellent multifractal scaling, certainly superior to the statistical scaling (see Subsection 3.3, as well as Fig. 8).

It was again striking to find such a clear difference between incoming and outgoing traffic. The characteristic difference between incoming, outgoing and combined traffic at CNET is best visible in an analysis of  $Z$ , i.e. ‘bytes per packets’. This time, the outgoing traffic yields very small  $\alpha$ , in fact only  $\alpha \leq 1$  and a ‘left-sided’ spectrum with only an increasing part, while the incoming and the combined traffic showed considerably less tendency towards burstiness (see Fig. 7). Traffic with a ‘left sided’ spectrum is very irregular, or ‘bursty’. Comparing with the findings for the traffic at Berkeley it has to be concluded that it is not necessarily the incoming traffic which contributes the bulk of the bursty traffic at the gateway of a LAN.

An explanation is offered by the fact that the bulk of the connections at CNET are contributed by World Wide Web connections. Here, the situation is more simple, or unbalanced, than at the complex LAN at Berkeley. A few clients in the LAN of CNET acknowledge the data received from the WWW interrupted by some sporadic sending of data, such as an email message. The outgoing traffic is, thus, sporadic, and bursty, though not of heavy load. The incoming traffic, on the other hand, has a more or less constant heavy flow with irregular but less violent behavior.

Indeed, the left-sided spectrum of the outgoing traffic reminds one rather of the spectrum of a Lévy stable motion than of the right-sided spectra of fractional Brownian motion (see [LR] and forthcoming publications). This is in perfect agreement with the ON/OFF model of Mandelbrot [ET] which leads in the limit to fractional Brownian motion for a ‘large’ number of sources, but to a Lévy process if only few sources are present.

Stationarity of data traffic is still an issue which is strongly discussed. It is clear that there is obvious non-stationarity due to human nature. It is, therefore, notable, that early morning hours as well as heavily loaded working hours show fairly similar multifractal spectra (see Fig. 7). In particular, the outgoing traffic at CNET is ‘left-sided’ at all times of various days which hints to a Lévy process as a model (see forthcoming publications).

### 3.3 Statistical versus multifractal scaling

Recall that the given positive data was denoted by  $Z_i$  and that

$$X_i := Z_i - \hat{\mathbb{E}}Z = Z_i - 1/N \sum_{i=1}^N Z_i.$$

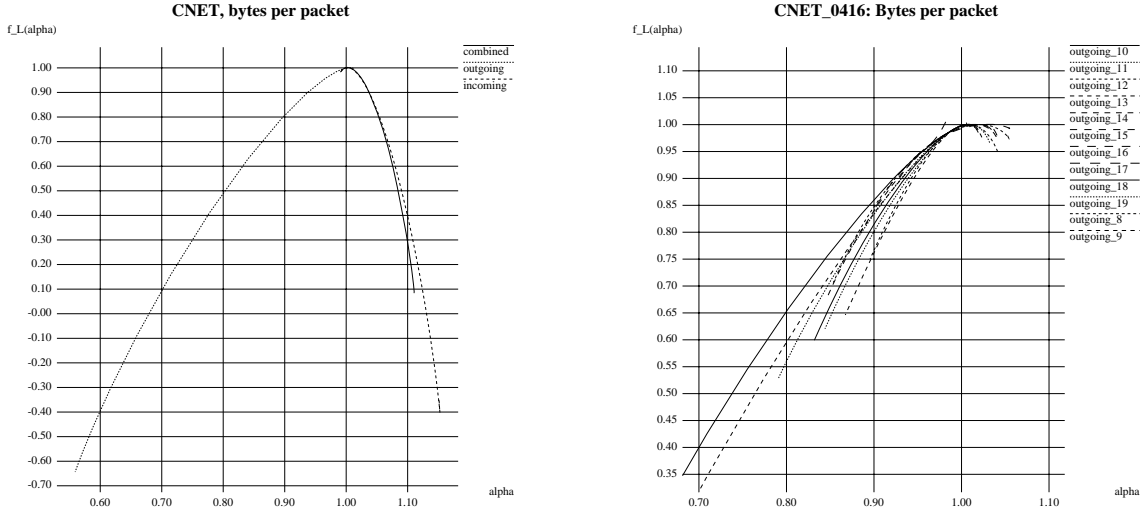


Figure 7: LEFT The Legendre spectra  $f_L$  of the ‘bytes per packets’ at CNET obtained using  $q = -4, -3.8, \dots, 4$ . For the outgoing traffic (dashed),  $f_L$  consists in a considerably broad increasing part. For the incoming as well as the combined traffic the  $f_L$  spectrum is ‘right sided’ and comparably narrow. RIGHT Spectra of the outgoing traffic at CNET at different hours of a day. Though there is obvious non-stationarity it is notable that the traffic is ‘left-sided’ at all times.

is the corresponding centered data. A multifractal analysis is in order for  $Z_i$  while a statistical analysis estimating the parameter of self-similarity  $H$  is suitable for  $X_i$ .

In order to compare the two scaling behaviors note that  $\sum_{k=1}^{N/m} X_k^{(m)} = 0$ , whence

$$S_m^Z(2) = \sum_{k=1}^{N/m} (\bar{Z}_k^{(m)})^2 = m^2 \sum_{k=1}^{N/m} (\bar{X}_k^{(m)} + m\hat{\mathbb{E}}Z)^2 = S_m^X(2) + mN(\hat{\mathbb{E}}Z)^2. \quad (14)$$

For the statistical estimator  $\hat{\mathbb{E}}|X^{(m)}|^q = (m^{1-q}/N)S_m^X(q)$  used in [TTW2] this translates to

$$\hat{\mathbb{E}}|Z^{(m)}|^2 = \hat{\mathbb{E}}|X^{(m)}|^2 + (\hat{\mathbb{E}}Z)^2$$

(the sample second moment equals the sample variance plus the sample mean squared).

At this point a conceptual difficulty arises. The statistical test looks for asymptotic behavior as  $m \rightarrow \infty$ , while multifractal analysis is formulated in terms of the limit  $\delta_m = m/N \rightarrow 0$ . The equation above shows now that scaling can’t be perfect for both simultaneously except in the trivial case  $\gamma(2) = \tau(2) = 1$ .

Nevertheless, the scaling behavior of both,  $S_m^Z$  and  $S_m^X$  may be acceptable in a *scaling region*, i.e. a range of values of  $m$  with nearly linear behavior in log-log coordinates. Some remarks are in order.

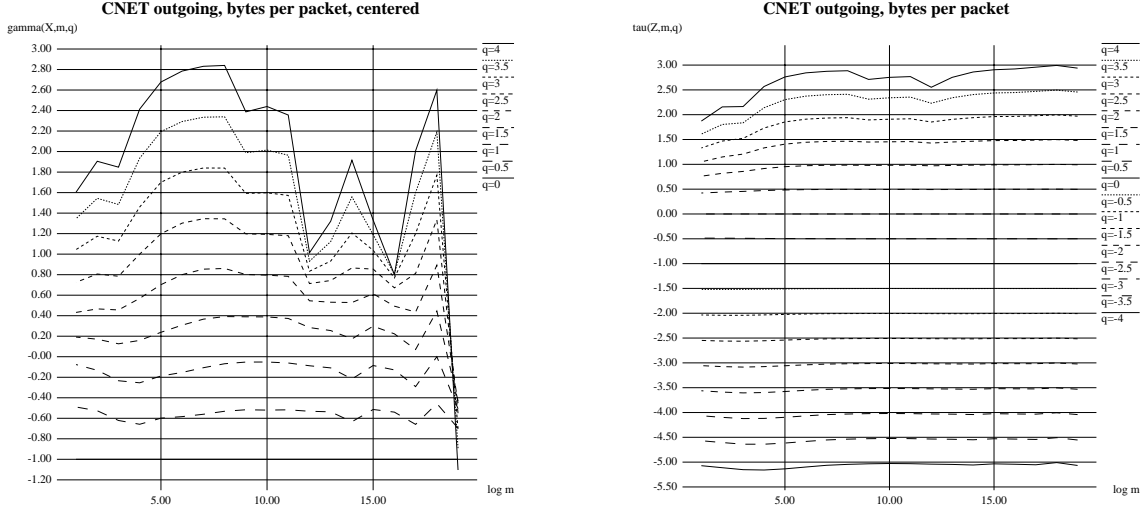


Figure 8: The superior scaling of non-centered data is most obvious when looking at the aspect  $B$  (bytes per packet) for the outgoing traffic at CNET, but the same behavior was found throughout the entire analysis (see, e.g. Fig. 4).

First,  $S_N^Z(q) = (S_N^Z(1))^q$  implies  $\tau_N^Z(q) \simeq q$ , while  $S_N^X(q) = 0 = \text{const}$  yields  $\gamma_N^X(q) \simeq 0$ . This forces the scaling to break down as  $m \rightarrow N$ . It is clear that the effect on  $\gamma_m^X$  is stronger since both,  $\tau$  and  $\gamma$  increase with  $q$  (see Fig. 4 and 8). In the limit  $m \rightarrow 1$ , on the other hand, imprecision of the measurement will affect the scaling behavior.

Second, being a rate function  $\tau(q)$  is convex. Since  $\tau(0) = -1$  and  $\tau(1) = 0$ , we must have  $\tau(2) \leq 1$ . On the other hand,  $\gamma(2) \leq 1$  follows from  $H \leq 1$ . Thus, the term of order  $m^1$  will not be essential for  $m \rightarrow 1$ .

All this makes clear that scaling should be expected rather in the multifractal limit  $m/N \rightarrow 0$ . If scaling is present there, (14) suggests

$$\tau(2) = \min(1, \gamma(2)) = \gamma(2) = 2H - 1. \quad (15)$$

Equation (15) illustrates, first of all, the way in which multifractal analysis goes beyond the ‘mono-fractal’ statistical tests based on an estimation of  $H$ . As an estimator of  $H$ , however,  $(\tau(2) + 1)/2$  is certainly of limited use. To illustrate this point in some detail, and in order to show what different conclusions a statistical and a multifractal approach allow, some estimations of  $H$  through  $\hat{H}_s := (\gamma(2) + 1)/2$  and  $\hat{H}_m := (\tau(2) + 1)/2$  have been calculated. As becomes apparent,  $\hat{H}_m$  is considerably larger than  $\hat{H}_s$  throughout the data. Table 1 illustrates, though, that one has to take the whole spectrum  $\tau(q)$  into consideration, not only one value such as  $\tau(2)$ .

With the statistical method of moments, finally, we encounter as an essential problem a general scaling behavior of a lesser quality, and more importantly, a significant dependence

$\hat{H}_m$	outgoing	incoming	combined
<b>Berkeley, <math>Z</math></b>	.981	.968	.983
<b>Berkeley, <math>B</math></b>	.957	.916	.952
<b>CNET, <math>Z</math></b>	.987	.998	.998
<b>CNET, <math>B</math></b>	.968	.937	.964

Table 1: The multifractal estimator  $\hat{H}_m = (\tau(2) + 1)/2$  of the Hurst exponent for the aspects  $Z$  (bytes per packet) and  $B$  (bytes per time). The other two aspects showed no conclusive difference between outgoing and incoming traffic. As this table illustrates, conclusions on the irregularity of data cannot rely on the value  $\tau(2)$  only. With the aspect  $B$  at CNET, e.g.  $\hat{H}_m$  suggests that the incoming traffic is more bursty than the outgoing one, a conclusion which is certainly denied when taking the whole spectrum into account (Fig. 7).

of the estimator on the choice of the scaling region (see Table 2). It has to be added in defense to this approach that despite of poor scaling the partition functions  $\gamma^B(q)$  and  $\gamma^T(q)$  of the centered aspects  $B$  and  $T$  are indeed fairly linear for  $q \geq -1$  up to values of  $q$  as large as 20. In other words, the corresponding Legendre transforms  $\gamma^*(\alpha)$  form an ‘edge’ at their maximum (Fig. 5). This linearity forms the basis of the statistical estimator of  $H$  and supports the conjecture of statistical self-similarity.

In summary, with the traces of this study the multifractal analysis is superior to the statistical method of moments for the following reasons:

- Throughout all data considered in this work, the multifractal scaling was more convincing.
- The necessary procedure of centering the data introduces inaccuracy in the statistical method of moments, whence the scaling is unacceptable for negative  $q$ .
- Essential properties concerning regularity and burstiness were found when looking at the whole spectrum and not only at one parameter.
- With the inter-arrival times  $T_i$  the properties just mentioned manifest themselves in the range corresponding to negative  $q$  and were, thus, even less accessible through the statistical method of moments.

## Conclusions.

The data traffic at Berkeley and at CNET labs both show indisputable multifractal behavior. Moreover, the scaling is extraordinary in both, quality and size of the scaling region.

$\hat{H}_s$	outgoing	incoming	combined
<b>Berkeley, <math>Z</math></b>	.828	.795	.832
<b>Berkeley, <math>T</math></b>	.835	.824	.843
<b>Berkeley, <math>B</math></b>	.800	.767	.775
<b>Berkeley, <math>P</math></b>	.790	.815	.790
<b>CNET, <math>Z</math></b>	.896	.876	.928
<b>CNET, <math>T</math></b>	.874	.771	.900
<b>CNET, <math>Z</math></b>	.915	.917	.924
<b>CNET, <math>T</math></b>	.926	.904	.926

Table 2: The statistical estimator  $\hat{H}_s$  for various aspects. The lines at the end are obtained from the same data (as indicated), however with different scaling regions  $2^5, \dots, 2^{10}$  as compared to  $2^1, \dots, 2^{18}$  which was applied at the top 6 lines (compare Fig. 8).

The latter is especially astonishing when compared to findings in other fields: the scaling region of TCP traffic spans four to five orders of magnitude as compared to the one to two orders which are typical in other fields. There is also evidence of statistical self-similarity, but notably only for  $q \geq 1$  and less convincing. Possible reasons for the high quality of the multifractal scaling are the hierarchy inherent to telecommunication protocols, as well as the fact that data transfers involve splitting wholes into pieces. Further support comes from the multiplicative approach to queueing as sketched in Subsection 2.2.

The multifractal analysis of the traffic, in particular the various spectra  $f_L$ , are best interpreted from a ‘distant point of view’. Rather than looking at the exact values  $f_L(\alpha)$  one looks at the shapes of the spectra. These spectra reveal telling information about the irregularities as well as regularities of the data traffic. E.g. it is possible to distinguish between incoming and outgoing traffic, as well as between the two LAN-s under investigation. Moreover, a more refined, direct measurement of (2) suggests that the incoming traffic at Berkeley consists of two largely independent ‘phases’ (Subsection 3.1).

With an estimation of the statistical parameter  $H$  (Table 2) such conclusion could not be drawn. In particular, when considered as a self-similar process the inter-arrival times are insensitive to the difference between incoming and outgoing traffic. To the contrary when treating this process as a multifractal. The main reason for this may be seen in the fact that the multifractal analysis captures also information about the inverse process, i.e. the traffic load, through the negative moments. But the inversion formula [MR, RM] holds for measures only, and not for general processes.

One could wonder which traffic, outgoing or incoming, should be more regular, both being subject to some smoothing effects: the incoming traffic comes from a WAN where a greater number of sources could lead to some averaging, while the outgoing traffic is produced by a LAN where response times are shorter and flow control should be more efficient. The

multifractal analysis, especially the comparison of the traffic at Berkeley and at CNET, shows that the very type of a LAN has a much greater influence than the mentioned effects. A tentative explanation of the very sporadic outgoing traffic at CNET could be found in the fact that the essential part of this traffic consists in WWW consultations of only a few clients which makes Lévy stable motion a more accurate model than fractional Brownian motion.

With random binomial measures (see Fig. 1) simple models of data traffic become available. Thereby, one should not fit a whole spectrum of scaling exponents  $\tau(q)$  to a given trace but rather adjust a few parameters which determine the distribution of the random weights  $M_0, M_1$  (Subsection 2.1) or more generally the distribution of the random multipliers (7). The model used in Fig. 1, e.g. has no parameter and was obtained by taking  $M_0 \simeq U[0, 1]$ ,  $M_1 := 1 - M_0 \simeq U[0, 1]$ . It is clear that this is too simple a model. The more astonishing is the visual similarity with an actual trace.

Several tasks lay ahead. First, it would be useful to calculate essential statistical information such as forecasting for such random measures, or multifractal processes. The knowledge of the whole multifractal spectrum will then allow more precise statistics than the knowledge of one scaling or ‘burst’ exponent  $H$  only. Secondly, ‘physically’ relevant models with multifractal properties going beyond Subsection 2.2 are needed for a better understanding of TCP traffic. These issues will be addressed in forthcoming papers.

## Acknowledgment.

We gratefully acknowledge the financial support of CNET, France, under contract # 95 8B 069. We would like to express our thanks to Fabrice Clerot and Ilkka Norros for useful comments on an earlier version of this paper.

## References

- [AP] M. ARBEITER AND N. PATZSCHKE, Self-Similar Random Multifractals, *Math. Nachr.* **181** (1996) pp 5–42.
- [Ell] R. ELLIS, Large Deviations for a general Class of Random Vectors, *Ann. Prob.* **12** (1984) pp 1–12.
- [ET] M. TAQQU AND J. LEVY, in *Dependence in probability and statistics*, (*Progress in probability and statistics*), vol. 11, p 73–89, E. Eberlein and M. Taqqu (eds.), Birkhaeuser Boston, Basel, Stuttgart (1996), ISBN 0-8176-3323-5.

- [EM] C. J. G. EVERTSZ AND B. B. MANDELBROT, Multifractal Measures, *Appendix B in: 'Chaos and Fractals' by H.-O. Peitgen, H. Jürgens and D. Saupe*, Springer New York (1992) pp 849–881.
- [F] K. J. FALCONER, *Fractal Geometry: Mathematical Foundations and Applications*, John Wiley and Sons, New York (1990).
- [GP] P. GRASSBERGER AND I. PROCACCIA, Measuring the strangeness of strange attractors, *Physica D* **9** (1983) pp 189–208.
- [HJKPS] T. HALSEY, M. JENSEN, L. KADANOFF, I. PROCACCIA AND B. SHRAIMAN, Fractal measures and their singularities: The characterization of strange sets, *Phys. Rev. A* **33** (1986) pp 1141–1151.
- [LTWW] W. LELAND, M. TAQQU, W. WILLINGER, AND D. WILSON, On the self-similar nature of Ethernet Traffic (extended version), *IEEE/ACM Transactions on Networking* (Feb. 1994) pp 1–15.
- [LV] J. LÉVY VÉHEL, Fractal Approaches in Signal Processing, *Fractal Geometry and Analysis, The Mandelbrot Festschrift, Curacao 1995*, C.J.G. Evertsz, H.-O. Peitgen, R.F. Voss (eds.), World Scientific, 1996.
- [LR] J. LÉVY VÉHEL AND R. RIEDI, Fractional Brownian Motion and Data Traffic Modeling: The other End of the Spectrum, *Fractals in Engineering*, Springer 1997, pp 185–202
- [M1] B. B. MANDELBROT, Intermittent turbulence in self similar cascades : divergence of high moments and dimension of the carrier, *J. Fluid. Mech.* **62** (1974) p 331.
- [M2] B. B. MANDELBROT, Negative Fractal Dimensions and Multifractals, *Physica A* **163** (1990) pp 306–315.
- [MR] B. B. MANDELBROT AND R. H. RIEDI, Inverse Measures, the Inversion formula and Discontinuous Multifractals, *Adv. Appl. Math.* **18** (1997) pp 50–58.
- [N1] I. NORROS, A storage model with self-similar input, *Queueing Systems* **16** (1994) pp 387–396.
- [N2] I. NORROS, On the use of fractional Brownian motion in the theory of connectionless networks, *COST/* **242** (1994).
- [NM] I. NORROS AND P. MANNERSLO, Multifractal analysis: A potential tool for teletraffic characterization?, *COST* **257** (1997) p 32.
- [P] V. PAXSON, Empirically-derived analytic models of wide-area TCP connections. *IEEE/ACM Transactions on Networking*, **2** (1994) 316–326.
- [R] R. H. RIEDI, An Improved Multifractal Formalism and Self-Similar Measures, *J. Math. Anal. Appl.* **189** (1995) pp 462–490.

- [RL1] R. RIEDI AND J. LÉVY VÉHEL, Multifractal Properties of TCP Traffic: a numerical study, *Technical Report 3129* INRIA Rocquencourt, (submitted January 1997). <http://www-syntim.inria.fr/fractales>
- [RM] R. H. RIEDI AND B. B MANDELBROT, Inversion formula for Continuous Multifractals, *Adv. Appl. Math.* **19** (1997) pp 332–354.
- [TTW1] M. TAQQU, V. TEVEROVSKY AND W. WILLINGER, Estimators for Long-Range Dependence: An empirical study, *Fractals.* **3** (1995) pp 785–798.
- [TTW2] M. TAQQU, V. TEVEROVSKY AND W. WILLINGER, Is the Ethernet data self-similar or multifractal?, *Fractals.* **5** (1997) pp 63–73.